Synchrotron X-ray Study of the Phase Transitions in Liquid Crystal Polyesters Derived from *p,p′*-Bibenzoic Acid and *racemic*- and (*R*)-3-Methyl-1,6-hexanediol

Ernesto Pérez,* Aránzazu del Campo, Antonio Bello, and Rosario Benavente

Instituto de Ciencia y Tecnología de Polímeros (CSIC), Juan de la Cierva 3, 28006 Madrid, Spain

Received November 15, 1999; Revised Manuscript Received January 28, 2000

ABSTRACT: The phase transitions in two liquid crystalline polyesters have been studied by diffraction techniques employing synchrotron radiation. The two polyesters, derived from *p,p′*-bibenzoic acid and 3-methyl-1,6-hexanediol, only differ on the optical activity of the chiral spacer: both the active and racemic polymers have been investigated. Time-resolved experiments at variable temperature were performed, analyzing the cooling from the isotropic melt and the subsequent melting. The analysis of the different diffraction profiles (covering WAXS, MAXS, and SAXS regions) shows important differences in the phase behavior of the two polyesters, more important than those anticipated from the analysis of the DSC curves. Nevertheless, a common feature is the obtention of S_C mesophases in both polymers, characterized by a continuous increase of the tilting angle as the temperature is decreased (before the appearance of high-order mesophases).

Introduction

The standard smectic chemical structure in thermotropic main chain polymers consists of regular alternating sequences of polar aromatic and nonpolar aliphatic building blocks, which promote an assembly of neighboring polymer chains forming a layer structure in a more or less perpendicular array relative to the polymer chains. From this point of view, the smectic phase formation may be interpreted as a phase separation on the nanometer level of the aromatic cores from the flexible spacers. The structures of the core and the spacer may influence the phase separation, and the resulting mesophase symmetry constitutes an interesting feature to be analyzed.

Several works have been published concerning the thermotropic liquid crystal character of main chain polymers containing the biphenyl unit as mesogen and different methylenic[1−3] or oxymethylenic[1,4,5] spacers linked by ester or ether[6,7] groups. Depending on the nature of the spacer and linkage group, different phase behaviors of the resulting materials are found. All the polymers show a remarkable odd−even effect of the number of methylene units of the spacer on the transition temperatures and the associated enthalpy or entropy changes. Moreover, in most cases linear spacers with an even number of methylene units develop upon cooling a mesophase of S_A type,[8] while for odd spacers the S_{CA} symmetry is usually found.[9] S_C mesophases have been reported for some oxymethylene spacers[10,11] and hydrocarbonated spacers with methyl substituents.[3,12] Similar systems including two different aliphatic spacers distributed in a regular alternate fashion along the polymer backbone form different mesophases depending on the difference in the lengths of the two spacers.[13,14] All these effects have been explained as a consequence of the conformation of the spacer in the mesophase, which confines the arrangement of the mesogenic groups in the smectic layers.

We have previously reported[3] a preliminary study of the phase transitions of liquid crystalline polyesters derived from *p,p′*-bibenzoic acid and *racemic*- and (*R*)-3-methyl-1,6-hexanediol. This asymmetric substituted spacer seems to favor the appearance of tilted smectic structures, which are specially interesting in cases where the constituent molecules contain chiral atoms, because of their intrinsic ferroelectric properties.[15,16]

The high molecular weight of the polymers and the high transition temperatures make difficult the identification of the mesophases because of the lack of recognizable textures when observed between crossed polarizers and of sufficient X-ray measurements at elevated temperatures. For this reason, the thermal transitions in these polymers were carefully studied by performing time-resolved X-ray diffraction experiments at variable temperature, using synchrotron radiation. This method gives us the possibility of following the evolution of the different mesophases with the temperature by means of their diffraction pattern.[17] The influence of the optical activity of the diol and of the asymmetry introduced by the lateral group, with respect to the homologous polymer with a linear spacer, was also analyzed.

Experimental Section

The synthesis of the spacers and the polymers has been reported previously.[3] In summary, both the *racemic*- and (*R*)-3-methyl-1,6-hexanediol were prepared from the corresponding commercial 3-methyladipic acids. The polymers were synthesized by melt transesterification of diethyl *p,p′*-bibenzoate and the corresponding diol using isopropyl titanate as catalyst. The polyesters were purified by dissolving in chloroform and precipitating in excess methanol. The polymers obtained are named poly((*R*)-3-methylhexamethylene *p,p′*-bibenzoate), (*R*)-P6MeB, and poly((*R,S*)-3-methylhexamethylene *p,p′*-bibenzoate), (*R,S*)-P6MeB. The structural formula of the polymers is the following:

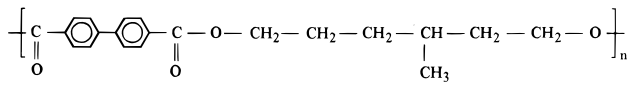

The intrinsic viscosities, molecular weights, and rotatory powers of the polymers are shown in Table 1.

10.1021/ma9919155 CCC: $19.00
Published on Web 03/24/2000

Table 1. Characterization of the Two Polybibenzoates

polymer	$[\eta]$ (dL/g)	$10^{-4}M_n$	M_w/M_n	$[\alpha]_D^{21}$ (rotatory power)
(*R*)-P6MeB	0.65	1.72	2.97	29.2
(*R,S*)-P6MeB	0.53	1.8	1.94	0

Differential scanning calorimetric measurements were carried out with a Perkin-Elmer DSC7 calorimeter connected to a cooling system. Samples of 8−10 mg were used.

X-ray scattering experiments were performed by employing synchrotron radiation ($\lambda = 0.150$ nm) in the beamline A2 at HASYLAB (Hamburg, Germany). Two linear position-sensitive detectors were used simultaneously: one of them fixed and covering the approximate 2θ range from 10° to 30° and the other being set at two different sample−detector positions (in the direction of the beam), 43 and 225 cm, respectively. The first position covers the approximate 2θ range from 1.1° to 8.8° (spacings from 8 to 1 nm), and the second, from about 0.18° to 1.6° (spacings from about 50 to 5.5 nm). Therefore, wide- (WAXS), middle- (MAXS), and small-angle scattering (SAXS) data are collected in the two experimental setups: simultaneous WAXS/MAXS profiles are acquired in the first case and WAXS/SAXS in the second.

Film samples, of about 20 mg, were covered by aluminum foil, to ensure homogeneous heating or cooling, and placed in the temperature controller of the line, under vacuum. Heating or cooling experiments were performed at rates of 2 or 4 °C/min. The same temperature programs were reproduced in the two setups, and the WAXS data were used to monitor the reproducibility of the results. The reproducibility was found to be well inside the inherent experimental resolution of the system. Moreover, no damage seems to be produced in the samples, since the phase transitions appear at exactly the same temperatures even after 5 or 6 melting−cooling cycles.

The scattering patterns were collected in time frames of 30 and 60 s for the rates of 4 and 2 °C/min, respectively, so that we have a temperature resolution of 2 °C between frames. The calibration of the spacings for the different detectors and positions was made as follows: the diffractions of a crystalline PET sample were used for the WAXS detector, a sample of a polyesterimide (giving a well-defined diffraction at a spacing of 2.81 nm) and a grid with separations of 5 mm were used for the MAXS detector, and the different orders of the long spacing of rat-tail cornea ($L = 65$ nm) were used for the SAXS detector.

Results and Discussion

Thermal Transitions. The thermal transitions of the two polybibenzoates have been first analyzed by DSC. The corresponding results are shown in Figure 1, where the upper part represents the cooling from the isotropic melt and the lower one the subsequent melting. Three exotherms are observed in both polymers when cooling from the isotropic melt. Their temperatures and enthalpies are presented in Table 2. It can be seen that the behavior on cooling is rather similar for the two polyesters. Thus, the same phase sequence seems to be anticipated from the DSC results, with the only important difference of a considerably higher temperature for the final transition in the optically active polymer.

The melting curves are, however, quite different, since only one endotherm is found for (*R*)-P6MeB ($T_m = 155.7$ °C, $\Delta H = 33.8$ J/g), suggesting a monotropic behavior for this polymer, similarly to the case of other polybibenzoates.[1,18,19] On the contrary, a melting curve composed of at least two peaks is observed for the racemic polymer, although the total enthalpy of melting (31.4 J/g) is only slightly lower than that for the optically active polybibenzoate.

The glass transition can be also observed in the two polymers. It appears at 26 and 32 °C respectively for (*R,S*)-P6MeB and (*R*)-P6MeB (in the melting experiments).

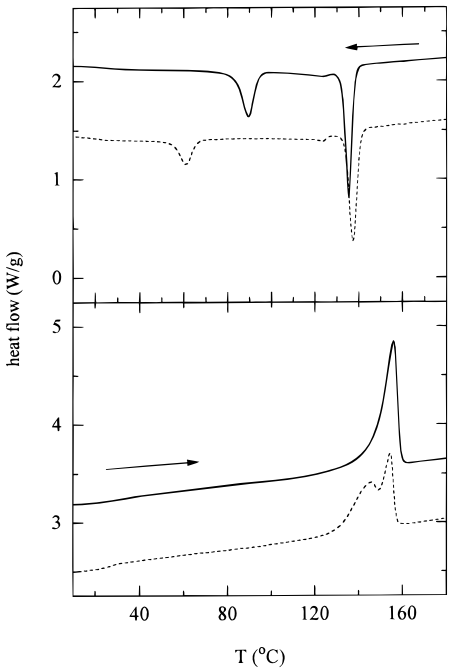

Figure 1. DSC curves corresponding to (*R*)-P6MeB (continuous lines) and (*R,S*)-P6MeB (dashed lines) in a cooling from the isotropic melt (upper) and the subsequent melting (lower).

Table 2. Temperatures and Enthalpies for the Different Transitions of the Two Polybibenzoates in a Cooling Experiment (at 20 °C/min)

polymer	T_1 (°C)	ΔH_1 (J/g)	T_2 (°C)	ΔH_2 (J/g)	T_3 (°C)	ΔH_3 (J/g)
(*R*)-P6MeB	135.5	15.6	123.8	3 ± 3	89.4	10
(*R,S*)-P6MeB	137.3	16.3	123.7	5 ± 2	60.9	6.2

Therefore, some differences in the phase behavior of the two polybibenzoates are deduced from the DSC experiments. The exact nature of the phases involved is studied below by using synchrotron radiation.

MAXS−WAXS Synchrotron Results. (a) *(R)*-P6MeB. The diffraction profiles corresponding to sample (*R*)-P6MeB in a cooling experiment from the melt are presented in Figure 2, showing the data acquired simultaneously in the two detectors. The profiles for the subsequent melting of this sample are shown in Figure 3. A careful analysis of all these profiles allows one to obtain a lot of quantitative information. Thus, it can be observed that at high temperatures an isotropic melt is obtained, characterized by the absence of peaks in the MAXS region and by the typical amorphous halo in the WAXS channels, centered at 0.49 nm. On lowering the temperature, the MAXS detector shows the appearance of a peak centered at around 1.9 nm, while the corresponding WAXS diffractograms are very similar to those of the isotropic melt. These features are characteristic of a low-order smectic phase. The MAXS peak appears at a temperature about 150 °C, showing a rapid increase of its intensity, as shown in the middle part of Figure 4. Regarding the WAXS diffractograms during this transition, a careful analysis shows that the center of the wide halo experiences, besides the expected thermal expansion, a clear discontinuity at a temperature of about 146 °C, as shown in the upper part of Figure 4, changing from around 0.49 nm for the isotropic phase to about 0.47 nm for the smectic one.

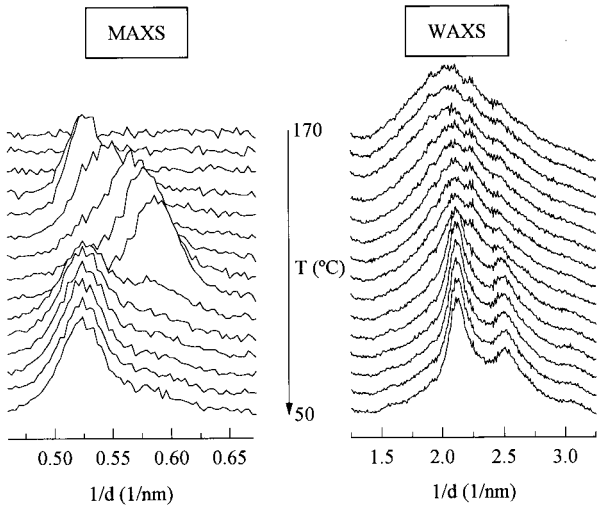

Figure 2. Scattering profiles corresponding to (*R*)-P6MeB in a cooling experiment from the isotropic melt. For clarity, only one of every four frames is plotted. Noticeable noise signals are present in the WAXS channels at around 2.25 and 2.50 nm^{-1}.

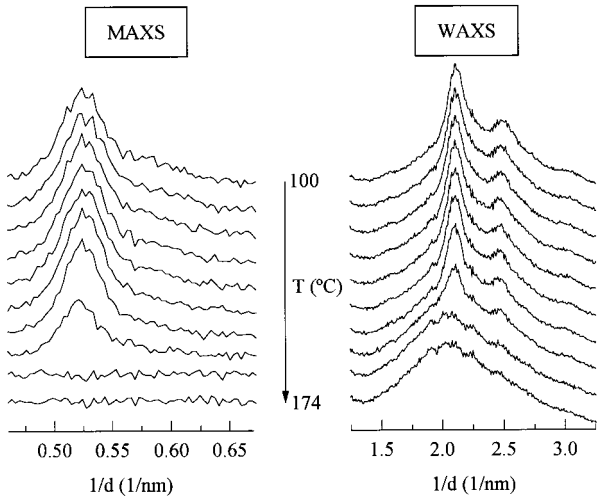

Figure 3. Scattering profiles corresponding to (*R*)-P6MeB in a melting experiment. For clarity, only one of every four frames is plotted.

After a few frames, the MAXS peak begins to shift to lower spacings, from a maximum value of 1.88 nm to a final value of 1.69 nm at a temperature of 105 °C (see left-hand side of Figure 2 and lower part of Figure 4). This shifting is accompanied by a slight increase of the total MAXS area, as shown in the middle part of Figure 4. No change is observed, however, in the WAXS diffractograms, with the exception, as usual, of a slight linear decrease of the position of the wide peak (see upper part of Figure 4), due to the thermal contraction. Therefore, we are dealing with a low-order mesophase. Previous WAXD results at room temperature on stretched samples of (*R*)-P6MeB quenched from the melt[3] indicated the presence of a S_C* structure in this polymer. This is consistent with the results in the present work; i.e., a smectic phase with the chain axis normal to the smectic planes is formed first, and later a tilting of the angle between the chain and the normal to those planes is produced, leading to a S_C* mesophase, which can be quenched at room temperature.

However, under the slow-cooling conditions of the present experiments, the S_C* phase experiences a

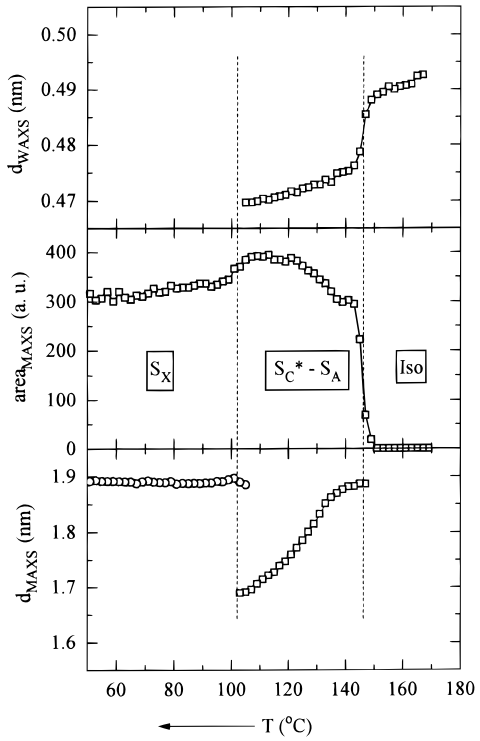

Figure 4. Variation of the position of the WAXS broad peak and of the total area and position of the MAXS peak as a function of temperature corresponding to (*R*)-P6MeB in the cooling experiment of Figure 2.

transition into a more ordered phase. Thus, at a temperature about 105 °C, the MAXS peak at around 1.7 nm diminishes in intensity, while a new one at around 1.9 nm is formed, remaining approximately at the same position until the end of the experiment. It is important to notice that the peak at 1.7 nm does not disappear completely, since a small shoulder is observed in the last frames.

The appearance of the final MAXS peak at 1.9 nm is accompanied by a small decrease of the total MAXS area (see middle part of Figure 4) and by a very clear change in the WAXS profiles, since two diffraction peaks, corresponding to spacings of 0.469 and 0.400 nm, are observed. Taking into account this feature and the fact that the MAXS spacing is similar to that of the S_A structure, that phase, which will be named S_X, may be an upright mesophase with, probably, orthorhombic symmetry and herringbone arrangement of the polymer molecules (S_E).

The transition temperatures deduced from the synchrotron results can be compared with the corresponding DSC ones. Figure 1 (and Table 2) shows the DSC transitions obtained at a cooling rate of 20 °C/min. (This rate has been chosen in order to get a better determination of the enthalpies involved in the different transitions, which are rather small, as seen in Table 2.) Obviously, the transition temperatures will depend on the cooling rate. Thus, Figure 5 shows the variation of the three transitions with the cooling rate. The values obtained at a cooling rate of 4 °C/min are practically coincident with those from the synchrotron results, deduced from Figure 4, if we consider that the exotherm centered at 130 °C corresponds to the maximum slope in the variation of the position of the MAXS peak during the formation of the S_C* phase.

The subsequent melting of this sample is much less complicated, as observed in Figure 3. The WAXS and

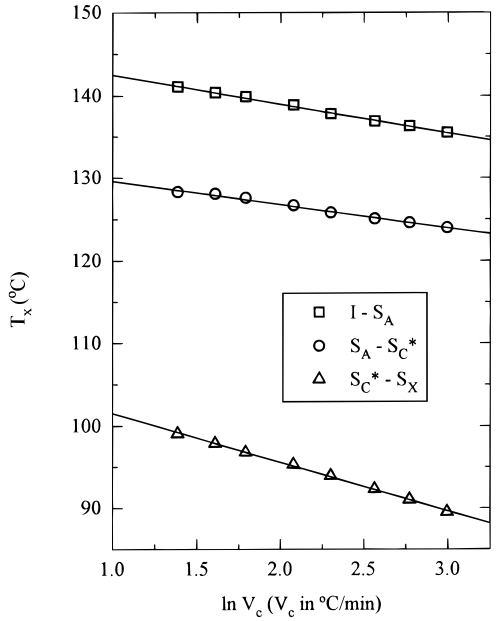

Figure 5. Dependence of the DSC peak transition temperatures with the cooling rate corresponding to (*R*)-P6MeB.

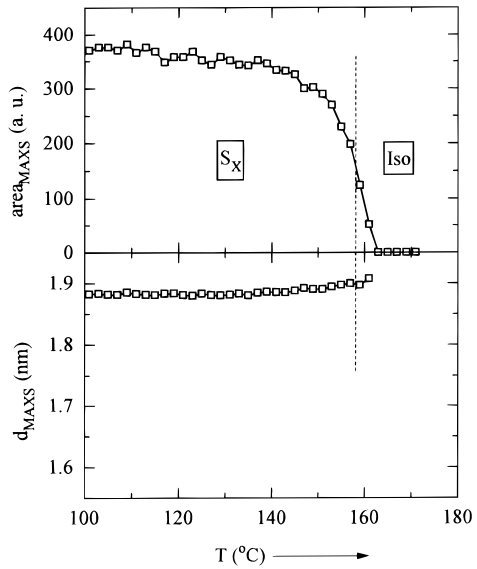

Figure 6. Variation of the total area and position of the MAXS peak as a function of temperature corresponding to (*R*)-P6MeB in the melting experiment of Figure 3.

MAXS profiles remain approximately the same until a temperature of about 160 °C, when the isotropization of the sample is observed. The data analysis is shown in Figure 6. These results indicate that the S_X phase experiences a monotropic melting, i.e., it melts directly into the isotropic phase, and the low-order smectic phases (S_A and S_C*) are not obtained on melting.

There is, however, one aspect to be commented on. It seems that a minor amount of S_C* phase remains untransformed, judging from the small shoulder centered at around 1.68 nm which is present in the MAXS profiles (see Figures 2 and 3). This shoulder may involve as much as 20% of the total MAXS peaks area, but it is not possible to analyze its behavior on melting with enough accuracy to extract any useful information.

***(R,S)*-P6MeB**. The phase behavior of the racemic polymer presents more differences in relation to the active polymer than those that can be anticipated from

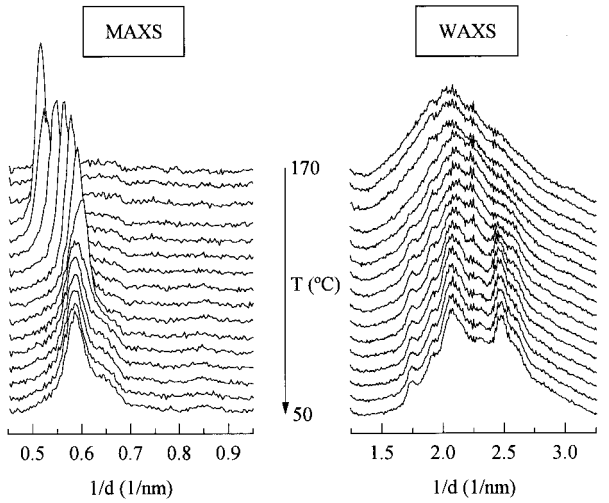

Figure 7. Scattering profiles corresponding to (*R,S*)-P6MeB in a cooling experiment from the isotropic melt. For clarity, only one of every four frames is plotted.

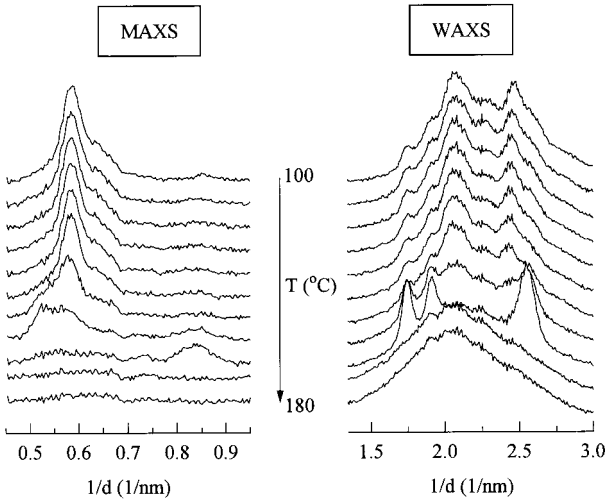

Figure 8. Scattering profiles corresponding to (*R,S*)-P6MeB in a melting experiment. For clarity, only one of every four frames is plotted.

the DSC analysis. Thus, Figure 7 shows the MAXS−WAXS profiles corresponding to the cooling of (*R,S*)-P6MeB from the isotropic melt, while the profiles corresponding to the subsequent melting are presented in Figure 8.

It can be observed that the first part of the cooling experiment is rather similar to that for the optically active polymer. Thus, at high temperatures only the isotropic phase is present: no MAXS peaks and a broad amorphous-like halo in the WAXS region, centered at 0.49 nm. On lowering the temperature, a S_A phase is formed at around 155 °C, characterized by a MAXS peak at 1.91 nm and a wide profile in the WAXS region, centered at 0.47 nm, clearly different from the value for the isotropic phase (see upper part of Figure 9).

At lower temperatures, the transition from S_A to S_C is also observed, but below 128 °C a minor amount of a highly ordered crystalline phase is formed, characterized by three distinct diffraction peaks in the WAXS region and by a MAXS peak at 1.18 nm, well different from the spacings of the smectic peaks. The fraction of this crystalline phase is very small, as determined from the area of those three diffraction peaks in relation to the total WAXS area: of the order of 3%, as shown in the

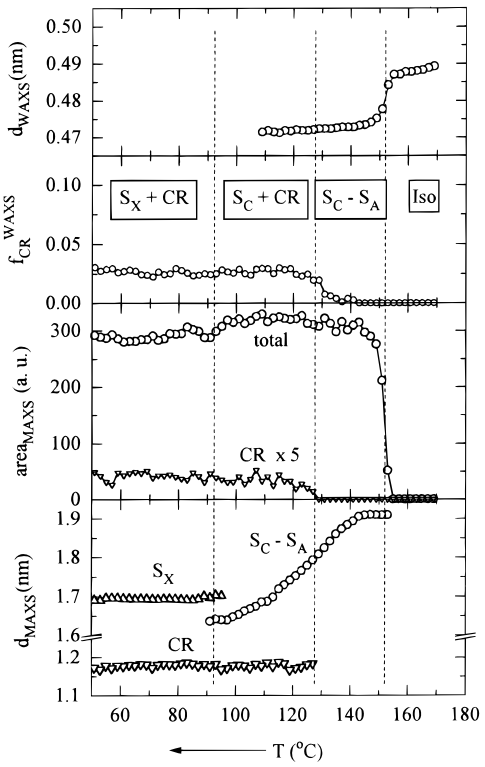

Figure 9. Variation of the position of the WAXS broad peak, of the fraction of crystal phase deduced from WAXS, and of the area and position of the MAXS peaks as a function of temperature corresponding to (*R*,*S*)-P6MeB in the cooling experiment of Figure 7.

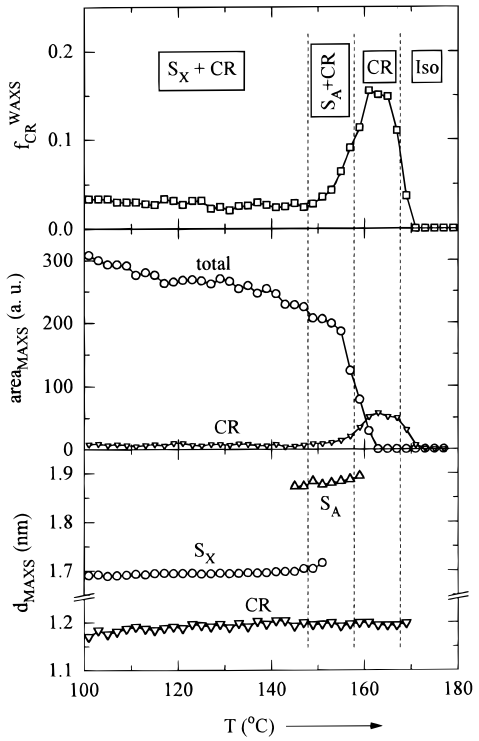

Figure 10. Variation of the fraction of crystal phase deduced from WAXS and of the area and position of the MAXS peaks as a function of temperature corresponding to (*R*,S)-P6MeB in the melting experiment of Figure 8.

second from the top part of Figure 9. The relative area of the corresponding MAXS peak is also about 3% of the total (see third from the top part of Figure 9).

Curiously, the proportion of this crystalline phase remains approximately constant even when going through the transformation of the S_C phase into the S_X one, which occurs in this polymer around 92 °C, as observed in the lower part of Figure 9. Here we find another difference between the two polymers: the MAXS peak of the S_X phase of (*R*,*S*)-P6MeB is centered at 1.7 nm; i.e., the MAXS spacing of this phase is much smaller than that for the corresponding phase of the optically active polymer. The two WAXS diffractions appear at 0.485 and 0.415 nm, i.e., slightly different than those for the active polymer. Therefore, we are dealing with a tilted mesophase of, probably, monoclinic symmetry and herringbone arrangement of the molecules (S_H or S_K).

The analysis of the subsequent melting experiment is shown in Figure 10. The situation now is quite different from that for (*R*)-P6MeB (compare with Figure 8): first, the S_X phase does not melt directly into the isotropic phase, since the S_A phase is observed in the temperature range from about 145 to 160 °C; i.e., the racemic polymer displays enantiotropic behavior on melting. Moreover, and simultaneously with the isotropization of the S_A phase, there is a very important recrystallization process, in such a way that the proportion of the crystalline phase increases from the initial 3% to a value of 15%, as shown in the upper part of Figure 10. The crystalline MAXS peak also experiences a parallel increase (see middle part of Figure 10). Finally, the melting of the crystals is attained at a temperature around 170 °C, leading to an isotropic phase.

In conclusion, and contrary to the case of (*R*)-P6MeB, the racemic polybibenzoate presents a phase behavior complicated by the fact of the appearance of a crystalline phase, in competition with the smectic ones. The relative proportion of them will depend very much on the crystallization conditions. Moreover, the recrystallization on melting will depend, as usual in this kind of process, on the heating rate. We have not carried out such analysis in the synchrotron source, but a rather good idea can be deduced from the DSC experiments displayed in Figure 11, where the melting curves at different heating rates and after two crystallization conditions are shown. Considering the synchrotron results, the endotherm at about 160 °C is attributed to the melting of the final crystals, and it is evident that the crystal phase is obtained in higher proportions the lower are the cooling and the heating rates. This phase, which is expected to be the most stable one, may be, therefore, the predominant one if very small rates are used (smaller than the 2 °C/min employed, for practical reasons, in the present experiments). Moreover, if the experiment represented by the upper curve in Figure 11 is stopped at 153 °C (after the formation of the crystalline phase and just before its melting) and cooled slowly from that state, the subsequent melting shows only the endotherm at about 160 °C; i.e., the crystalline phase seems to be the only one present under those conditions.

SAXS−WAXS Results. A parallel analysis has been carried out, for both polymers, by acquiring the scattering in the SAXS region (simultaneously with the WAXS region, which has been used to test the reproducibility of the phase transitions in relation to the MAXS−WAXS experiments).

Figure 12 shows the Lorentz-corrected profiles corresponding to selected temperatures of (*R*)-P6MeB in a

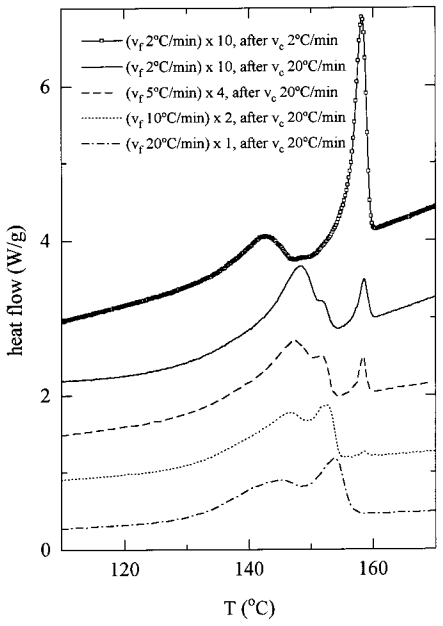

Figure 11. Dependence of the DSC melting pattern with the cooling, v_c, and melting, v_f, rates corresponding to (*R*,*S*)-P6MeB.

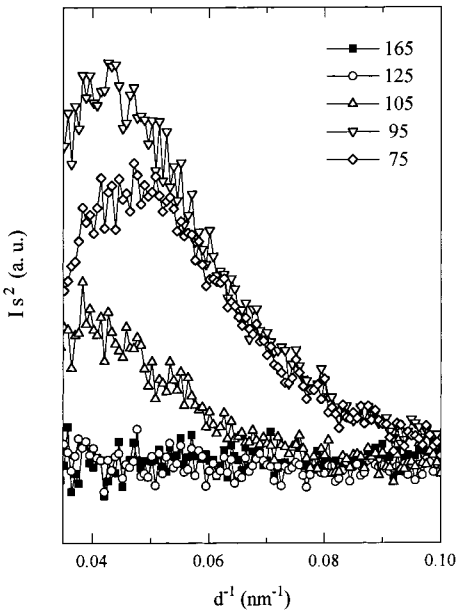

Figure 12. Lorentz-corrected SAXS profiles corresponding to selected temperatures of (*R*)-P6MeB in a cooling experiment.

cooling experiment. The scattering profiles for the isotropic melt (frame at 165 °C) and the low-order smectic phases, S_A (not shown) and S_C* (frame at 125 °C), are practically identical, but below 105 °C, and coinciding with the formation of the S_X phase, a long spacing is observed. Figure 13 shows the data derived from this experiment, compared to the corresponding one for the racemic polymer. The upper part of this figure shows the change of the relative invariant (the area under the SAXS curves[20]). For (*R*)-P6MeB a very clear increment of the invariant can be observed at about 105 °C, simultaneously with the appearance of a long spacing of around 20 nm. From these results and the WAXS characteristics, it can be deduced that the S_X phase presents a quasicrystalline degree of order.

The behavior of (*R*,*S*)-P6MeB on cooling from the melt shows also a clear increase on the invariant (see upper

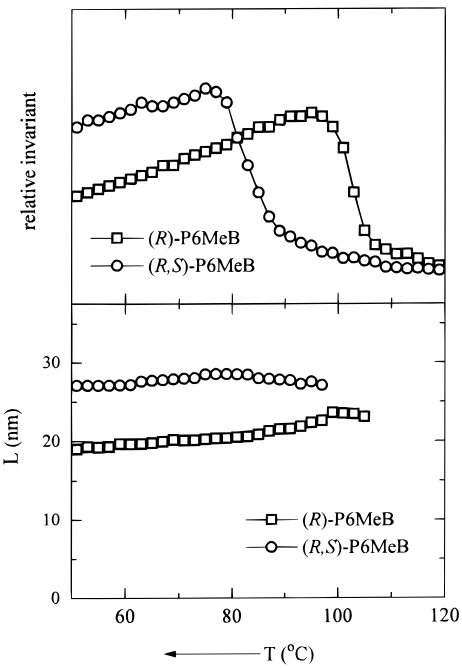

Figure 13. SAXS data (relative invariant and long spacing) as a function of temperature for the two polymers on cooling from the isotropic melt.

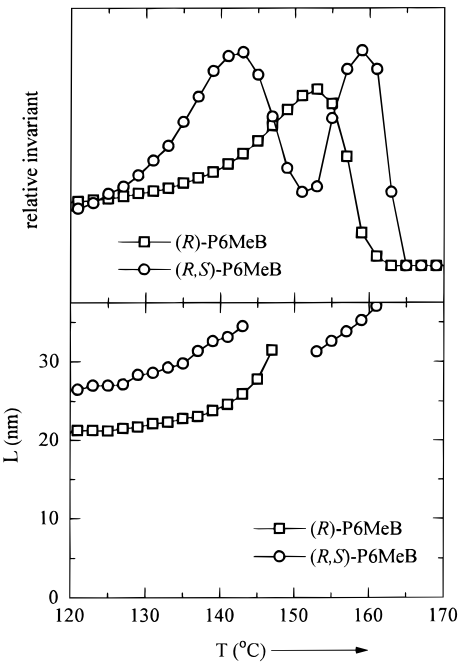

Figure 14. SAXS data (relative invariant and long spacing) as a function of temperature for the two polymers on melting.

part of Figure 13) at a temperature around 85 °C, i.e., when the S_X phase of this polymer is formed (see Figure 9). However, the long spacing is already observed at higher temperatures, due to the fact of the formation of the small amount of crystalline phase.

The SAXS data derived from the subsequent melting experiments for both polymers are presented in Figure 14. Regarding the optically active polymer, its behavior is again quite simple: after a steady increase of the invariant, there is a rapid decrease at about 158 °C, due to the monotropic isotropization of the S_X phase. The long spacing experiences a parallel increase (which cannot be measured above 147 °C when it raises to more

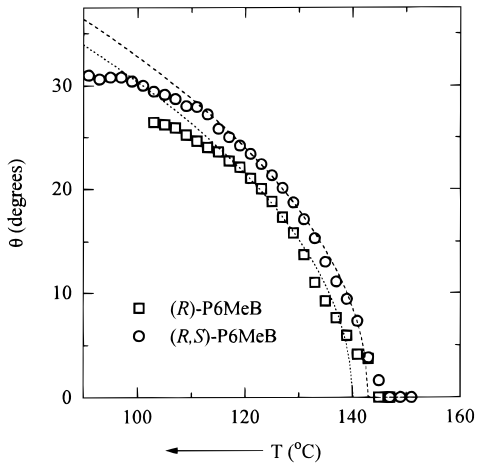

Figure 15. Variation of the tilt angle of the S_C phase of the two polymers with temperature in a cooling experiment. The dashed lines correspond to the fitting to eq 1, with the parameters indicated in the text.

than 30 nm, since it goes out of the detection window) before its final disappearance when the isotropization of the sample occurs.

The data corresponding to the racemic polymer reflect very clearly the recrystallization phenomena: there are two maxima in the invariant. Moreover, the long spacing, which disappears in a certain interval around 150 °C, shows up again when the sample experiences the important recrystallization process at around 155 °C. The isotropization of the sample is finally obtained above 165 °C.

Comparison of the Structural Parameters of the Two Polymers. As we have seen, the phase behavior of the two polymers presents important differences, although some of the structural parameters are similar. This is the case of the most probable distance found for the isotropic melt and for the low-order smectics in the WAXS region: around 0.49 nm for the isotropic phase and 0.47 nm for the low-order smectic phases, for both polymers.

Regarding the length of the smectic layers, it is around 1.9 nm for the S_A phase of the two polymers, and the angle of inclination in the S_C phase is also rather similar, as shown in Figure 15: it takes a value close to 30° at about 100 °C for both polymers. The difference is that the racemic polymer reaches a higher value of the angle, mostly because of its lower temperature for the formation of the S_X phase.

According to the Landau−de Gennes theory, the second-order transition from S_A to S_C can be described by the continuous increase of the tilt angle, θ (taken as the order parameter of the transition), in such a way that the free energy can be expressed in terms of powers of the tilt angle.[21] In such case, and neglecting the higher powers of θ, i.e., for temperatures not far away from T_C (the temperature at which the tilt appears), the following equation is obtained:

$$\theta = k(T_c - T)^{0.5} \qquad (1)$$

where k is a constant. This relation has been checked[22] for LMWLC as well as for polymeric liquid crystals. In our case, as depicted in Figure 15, this parabolic function describes rather well the temperature behavior of our data, with $k = 4.8$ and 5.0 and $T_C = 140$ and 143 °C, for (*R*)-P6MeB and (*R*,*S*)-P6MeB, respectively. As expected, the range of validity of that equation is restricted to temperatures not very much below T_C.

Finally, regarding the S_X phases, they are characterized by two WAXS diffractions at 0.469 and 0.400 nm for (*R*)-P6MeB and at 0.485 and 0.415 nm for the racemic polymer; i.e., they are also very close, although the spacings for the optically active polymer are about 3% smaller than for the racemic polybibenzoate. The difference lies, however, in the MAXS spacing, which is around 1.9 nm for (*R*)-P6MeB and only 1.7 nm for the racemic polymer. Comparing with the spacings of the S_A phase, it seems that we have an upright phase in the first case, and it is inclined for the second polymer.

Anyway, the most important difference in the phase behavior of the two polybibenzoates studied here is the capability of the racemic polymer for forming a three-dimensional crystalline structure, which is not present (at least under the experimental conditions used) in the optically active polymer, despite the fact of a greater structural regularity in the latter polybibenzoate.

If we compare now the behavior of these polybibenzoates with that for the corresponding polymer with a linear, nonsubstituted, spacer, i.e., with poly(hexamethylene *p*,*p*′-bibenzoate), PB6, it can be deduced that the presence of the methyl substituent has a very important effect on the transition temperatures, since the isotropization temperature of PB6 is of the order[23] of 240 °C. Moreover, the phase behavior is also quite different: PB6, on cooling from the melt, leads to a S_A mesophase, which is transformed into a crystalline structure on further cooling. However, the methyl groups, as we have seen, favor the appearance of S_C mesophases (where the accommodation of the methyls into the mesophase structure is achieved by tilted association of the polymer chains[12]), and the formation of crystalline structures is greatly inhibited.

Acknowledgment. The financial support of Fundación Ramón Areces and of the Comisión Interministerial de Ciencia y Tecnología (Project MAT98-061-C02-01) is gratefully acknowledged. The synchrotron work (in the polymer line of Hasylab at DESY, Hamburg) was supported by the TMR Contract ERBFMGECT950059 of the European Community. We thank the collaboration of the Hasylab personnel, especially Dr. A. Meyer, responsible for the polymer beamline.

References and Notes

(1) Pérez, E.; Pereña, J. M.; Benavente, R.; Bello, A. In *Handbook of Engineering Polymeric Materials*; Marcel Dekker: New York, 1997; Chapter 25.
(2) Watanabe, J.; Hayashi, M.; Morita, A.; Niiori, T. *Mol. Cryst. Liq. Cryst.* **1994**, *254*, 221.
(3) del Campo, A.; Pérez, E.; Benavente, R.; Bello, A.; Pereña, J. M. *Polymer* **1998**, *39*, 3847.
(4) Bello, A.; Pereña, J. M.; Pérez, E.; Benavente, R. *Macromol. Symp.* **1994**, *84*, 297.
(5) Bello, A.; Riande, E.; Pérez, E.; Marugán, M. M.; Pereña, J. M. *Macromolecules* **1993**, *26*, 1072.
(6) Shaffer, T. D.; Jamaludin, M.; Percec, V. *J. Polym. Sci., Polym. Chem. Ed.* **1986**, *24*, 15.
(7) Percec, V.; Shaffer, T. D.; Nava, H. *J. Polym. Sci., Polym. Lett. Ed.* **1984**, *22*, 637.
(8) Watanabe, J.; Hayashi, M. *Macromolecules* **1989**, *22*, 4083.
(9) Watanabe, J.; Kinoshita, S. *J. Phys. II* **1992**, *2*, 1237.
(10) Benavente, R.; Pereña, J. M.; Pérez, E.; Bello, A. *Polymer* **1994**, *35*, 3686.
(11) Heaton, N. J.; Benavente, R.; Pérez, E.; Bello, A.; Pereña, J. M. *Polymer* **1996**, *37*, 3791.

(12) Watanabe, J.; Hayashi, M.; Kinoshita, S. *Polym. J.* **1992**, *24*, 597.
(13) Watanabe, J.; Nakata, Y.; Simizu, K. *J. Phys. II* **1994**, *4*, 581.
(14) Nakata, Y.; Watanabe, J. *Polym. J.* **1997**, *29*, 193.
(15) Meyer, R. B.; Liebert, L.; Strzelecki, L.; Keller, P. *J. Phys., Lett.* **1975**, *36*, L-69.
(16) Watanabe, J.; Hayashi, M.; Morita, A.; Tokita, M. *Macromolecules* **1995**, *28*, 8073.
(17) Kricheldorf, Hans, R.; Probst, N.; Wutz, C. *Macromolecules* **1995**, *28*, 7990.
(18) Pérez, E.; Bello, A.; Marugán, M. M.; Pereña, J. M. *Polym. Commun.* **1990**, *31*, 386.
(19) Pérez, E.; Zhen, Z.; Bello, A.; Benavente, R.; Pereña, J. M. *Polymer* **1994**, *35*, 4794.
(20) O'Kane, W. J.; Young, R. J.; Ryan, A. J.; Bras, W.; Derbyshire, G. E.; Mant, G. R. *Polymer* **1994**, *35*, 1352.
(21) Lagerwall, S. T. *Ferroelectric and Antiferroelectric Liquid Crystals*; Wiley-VCH: New York, 1999.
(22) Watanabe, J.; Hayashi, M.; Nakata, Y.; Niori, T.; Tokita, M. *Prog. Polym. Sci.* **1997**, *22*, 1053.
(23) Tokita, M.; Takahashi, T.; Hayashi, M.; Inomata, K.; Watanabe, J. *Macromolecules* **1996**, *29*, 1345.

MA9919155